

Disc3D: Automatic Curation of High-Quality 3D Dialog Data via Discriminative Object Referring

Siyuan Wei¹ Chunjie Wang¹ Xiaosheng Yan¹ Rui Huang² Zhishan Zhou¹ Xiao Liu¹
¹PICO, ByteDance, Beijing
²Tsinghua University

{weisiyuan.buaa, wangchunjie01, yanxiaosheng, zhouzhishan.2013, liuxiao.ai}@bytedance.com
 hr20@mails.tsinghua.edu.cn

Abstract

3D Multi-modal Large Language Models (MLLMs) still lag behind their 2D peers, largely because large-scale, high-quality 3D scene–dialogue datasets remain scarce. Prior efforts hinge on expensive human annotation and leave two key ambiguities unresolved: viewpoint ambiguity—spatial language presumes unknown camera poses, and object referring ambiguity—non-exclusive descriptions blur the line between targets and distractors. We therefore present a fully automated pipeline that converts raw 3D scans into unambiguous, high-quality dialogue data at a fraction of the previous cost. By synergizing rule-based constraints with 2D MLLMs and LLMs, the pipeline enables controllable, scalable generation without human intervention. The pipeline comprises four stages: (1) meta-annotation collection harvesting object-, frame-, and scene-level captions, (2) scene graph construction with relation correction to capture the proximal object relations, (3) discriminative object referring that generates exclusive and compact descriptions, and (4) multi-task data generation synthesizing diverse dialogues. Our pipeline systematically mitigates inherent flaws in source datasets and produces the final Disc3D dataset—over 2 million samples in 25K hybrid 3D scenes, spanning scene&view&object captioning, visual grounding, and five object-centric QA tasks. Extensive experiments demonstrate that training with Disc3D yields consistent, significant improvements on both public benchmarks and our multifaceted Disc3D-QA tasks. Code, data, and models will be publicly available.

1. Introduction

Multi-modal understanding of 3D scenes is a prerequisite for embodied agents and robotic systems, yet current models lag far behind their 2D counterparts. A key bottleneck is the lack of versatile 3D vision foundation models, ex-

acerbated by the acute scarcity of large-scale, annotated 3D scene dialogues. Compared with 2D data, 3D modality incurs prohibitive collection and annotation costs, severely limiting the scale of datasets that can support training 3D Multi-modal Large Language Models (MLLMs).

Existing 3D MLLM datasets predominantly rely on manual annotation [1, 3, 8, 22, 23, 37, 42], which is inherently costly and limits scalability. Moreover, free-form annotations introduce two critical ambiguities: 1) *Viewpoint ambiguity*: As Fig. 1a shows, spatial descriptions often presuppose a specific 2D camera pose that is unknown during training and evaluation; 2) *Object referring ambiguity*: The unconstrained object referring expressions lack discriminative features, making target objects indistinguishable from distractors, as shown in Fig. 1b. Meanwhile, as Fig. 2 shows, inherent deficiencies in existing 3D scene datasets substantially increase the difficulty of multi-modal data generation. These issues necessitate an automated, systematic, scalable pipeline to convert raw scans into unambiguous, high-quality 3D dialogue data.

To tackle these challenges, we present the *Disc3D* dataset, which features a fully automated pipeline for generating high-quality 3D scene dialog data. The pipeline integrates 2D MLLM and LLM capabilities with rule-based processes at each stage, thereby leveraging the model’s capacity to perform automatic annotation under a controlled paradigm. Drawing inspiration from how humans identify an object’s distinctive features to resolve ambiguity in real-world conversations, we introduce *Discriminative Object Referring*. It enhances the dialogue’s contextual information by focusing on object referrals, reduces potential referring ambiguities, and increases the task’s complexity. Specifically, our pipeline consists of four stages:

1. **Meta-Annotation Collection**: Acquire scene-, image-, and object-level annotations by prompting 2D MLLMs to support subsequent multi-task generation.
2. **Scene Graph Construction**: Construct a spatial rela-

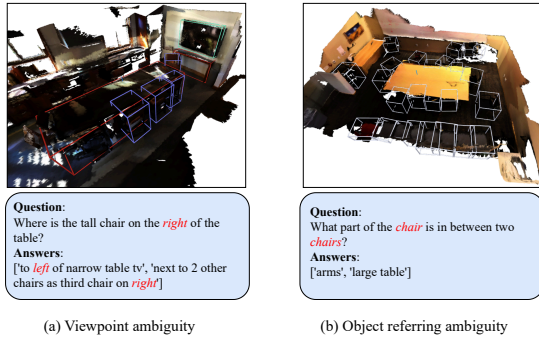


Figure 1. Examples of ambiguity in ScanQA, including (a) *viewpoint ambiguity*: the relative positions of objects (e.g., right or left) implied in a dialogue depend on viewpoint information not present in the context; and (b) *object referring ambiguity*: object descriptions (e.g., chair) lack discriminative detail, resulting in confusion between the target object and distractors.

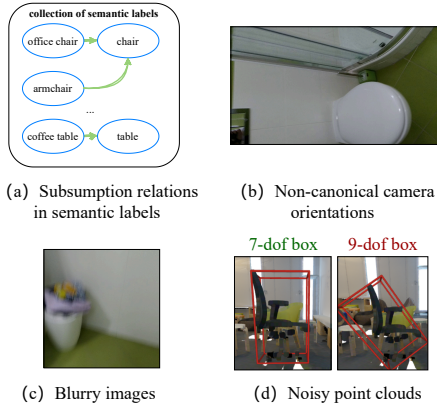


Figure 2. Common defects in 3D scene datasets that impede dialogue data generation: a) *Semantic label subsumption* (e.g., *office chair* vs. *chair*) induces referential ambiguity; b) *Non-canonical camera views* degrade 2D MLLM annotation accuracy; c) *Blurry images* reduce visual confidence; d) *Noisy point clouds* produce inaccurate 9-DOF boxes, impairing downstream learning.

relationship graph (objects as nodes) using rule-based methods, then refine it to correct errors arising from rule misjudgments as shown in Fig. 4a.

3. **Discriminative Object Referring:** Generate exclusive descriptions for each object along five dimensions to distinguish objects from possible distractors as shown in Fig. 4b.
4. **Multi-Task Data Generation:** Leverage the above information to produce diverse, context-rich dialogue data.

During production, we specifically address inherent issues in source datasets as shown in Fig. 2. Noting the absence of a fully open-source 3D MLLM data curation

pipeline, we will release our entire pipeline to foster community development. Utilizing this pipeline, we construct *Disc3D* dataset, as shown in Fig. 3, comprising millions of multi-task dialogue samples in 25K scans. We prove that training established 3D MLLM architectures on *Disc3D* yields promising improvements on our benchmark and other public benchmarks.

Our contributions are summarized as follows:

- We introduce a fully automated 3D scene dialog data curation pipeline. Centered on discriminative object referring, it generates context-rich, high-quality multi-task data while minimizing the impact of source dataset flaws and avoiding possible ambiguities.
- We present *Disc3D*, a million-scale dataset for training & evaluating 3D MLLMs, encompassing diverse and comprehensive range of task types.
- We re-implement one of state-of-the-art 3D MLLMs and utilize the *Disc3D* dataset for training. Extensive evaluations on *Disc3D* and other existing benchmarks show that our *Disc3D* dataset leads to substantial performance improvements.

2. Related Work

3D Multi-modal Datasets. Early work exploited 3D scene scans [5, 7, 11, 12, 25, 28, 31] to establish diverse 3D multi-modal benchmarks, including 3D question answering (QA) [3, 23, 24, 37] and 3D visual grounding [1, 8, 42]. 3D QA task assesses 3D MLLM’s understanding of objects and layouts in the scene [9, 15, 47], while 3D visual grounding tasks evaluate its ability to localize objects [10, 17, 21, 33, 35, 38, 41]. Motivated by advances in Large Language Models (LLMs) and 2D Multi-modal LLMs (MLLMs), more recent efforts [18, 22] combine human annotations with 2D MLLM capabilities to generate large-scale 3D scene data. However, these pipelines suffer from viewpoint ambiguity and referential uncertainty due to unconstrained annotations, and incur high production costs because of extensive manual labeling. We address these challenges with a fully automated pipeline based on Discriminative Object Referring, producing a larger, more diverse corpus free from previous ambiguities and cost constraints.

3D Multi-modal Large Language Models. Building on the rapid progress of 2D MLLMs [4, 30, 34, 45], recent research integrates 3D visual information into LLMs to create 3D MLLMs. Proposed methods include point-cloud modules [2, 13, 26, 36], lifted 2D foundation features [45], video-based representations [43], instance-level embeddings [40], and bird’s-eye-view projections [27]. Owing to the increased dimensionality and complexity of 3D data, no single architecture yet demonstrates robust spatial understanding from limited training samples.

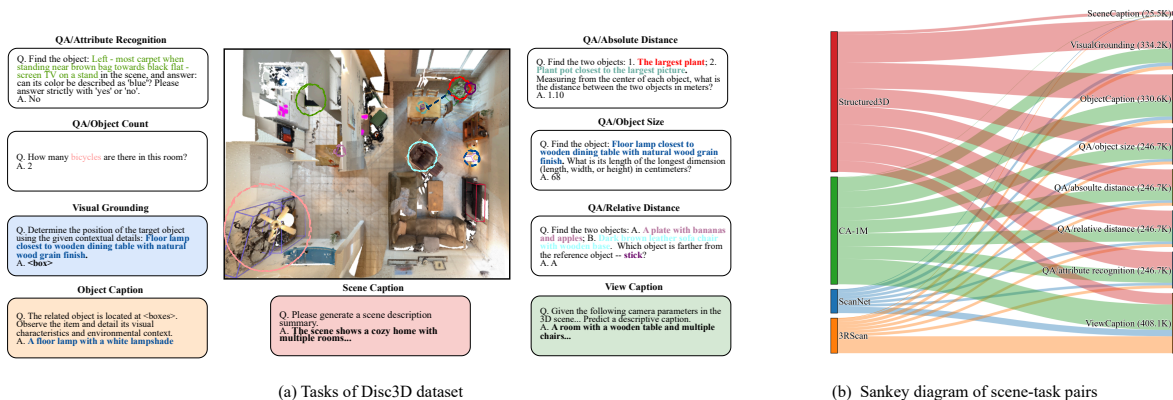


Figure 3. Overview of our Disc3D dataset. (a) Disc3D comprises millions of dialogue samples across 25K hybrid (real and synthetic) scenes, covering five object-centric QA tasks and three caption tasks for training & benchmarking 3D MLLMs. Object descriptions are color-coded to match the corresponding highlighted objects. (b) Task and scene distributions in the training set. The object counting task is excluded due to category-specific answer bias.

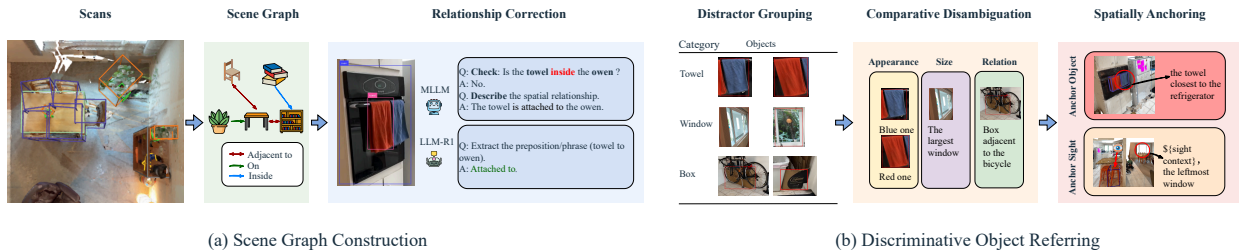


Figure 4. A schematic overview of two key stages in our data curation pipeline. Specifically: a) Scene Graph Construction proceeds in two stages: an initial graph is built automatically, after which a LLM & MLLM-guided module refines the misjudged relations (highlighted in red). b) Discriminative Object Referring produces exclusive, unambiguous descriptions for each object in the distractor group across five orthogonal axes. The first sub-stage, Comparative Disambiguation, contrasts objects of the same category along appearance, size, and relational cues; the second sub-stage, Spatially Anchoring, injects 3D context by explicitly conditioning every description on the designated anchor object or sight.

3. Dataset

This section first reflects on key issues in prior data work within the 3D MLLM domain. Next, we discuss the inherent flaws of existing 3D scene datasets that constrain data generation. We then describe our automated curation pipeline and conclude with a statistical profile and analysis of the resulting Disc3D corpus.

3.1. Reflections on Existing 3D MLLM Datasets

During our study of 3D MLLMs, we observed two major deficiencies in existing datasets as illustrated in Fig. 1:

- **Viewpoint Ambiguity:** Relative positional descriptions within the context (e.g., front/back, left/right) are tied to the camera viewpoint observed by the annotator or MLLM. While conventional references (e.g., adjacent walls) sometimes exist, the absence of explicit viewpoint information hinders the model training or evaluation in reasoning the spatial relationship.

- **Object Referring Ambiguity:** The unconstrained description (e.g., the object category or caption), when used for object referring, lacks exclusivity and may be confused with other objects in the scene.

3.2. Deficiencies in Source Data

Existing 3D scene datasets were not created with 3D MLLMs in mind, and their idiosyncrasies must be explicitly neutralised before they can be reused for multi-modal instruction tuning (Fig. 2). Two obstacles are particularly problematic:

- **Subsumption relations in semantic labels.** Class names often form a taxonomy: *dining table* is a hyponym of *table*. Treating every hypernym as a stand-alone label either forces the model to overlook valid hyponyms or invites context-level ambiguity when only the broader term is accepted as correct.
- **Non-canonical camera poses.** Arbitrary viewpoints–

Algorithm 1 Comparative Disambiguation

Input: The distractor group $O = \{o_1, o_2, \dots, o_n\}$.

Output: A mapping M from each object o_i to its descriptions.

```
1: # Step 1. Group objects via multi-aspect comparison
2: #  $G_{app}$ : appearance (e.g., 'red')  $\mapsto$  objects
3:  $G_{app} \leftarrow \text{GroupByAppearance}(O, \text{LLM})$ 
4: #  $G_{size}$ : size (e.g., 'the largest')  $\mapsto$  objects
5:  $G_{size} \leftarrow \text{GroupBySize}(O)$ 
6: #  $G_{rel}$ : object relations (e.g., 'beside the table')  $\mapsto$  objects
7:  $G_{rel} \leftarrow \text{GroupByRelations}(O)$ 
8:  $G_{all} \leftarrow \text{merge}(G_{app}, G_{size}, G_{rel})$ 
9: # Step 2. Assign exclusive and compact descriptions
10:  $C \leftarrow \{k \mid k \in G_{all}[k]\}$ 
11: for each object  $o_i \in O$  do
12:   Initialize  $D_i = \emptyset$  for object  $o_i$ 
13:   for each non-empty subset  $S \subseteq C$  do
14:      $U \leftarrow \bigcap_{k \in S} G_{all}[k]$ 
15:     if  $U = \{o_i\}$  then
16:        $d_S \leftarrow \text{", ".join(sorted}(S)}$ 
17:       Append  $d_S$  to  $D_i$ 
18:     end if
19:   end for
20:   # Keep only compact descriptions
21:   # (e.g., prefer "red" over "red, large").
22:    $M[o_i] \leftarrow \{d \in D_i \mid \text{is\_compact}(d)\}$ 
23: end for
24: return  $M$ 
```

especially those with large out-of-plane rotation—systematically degrade the quality of MLLM-generated annotations.

Because the label vocabularies differ across source corpora, we let a strong LLM [20] build a single directed graph that encodes the subsumption structure. Each node is an object label; a directed edge $u \rightarrow v$ exists whenever LLM confirms that v is a subtype of u (Fig. 2a). Candidate edges are first shortlisted by word overlap and then validated by LLM in a zero-shot fashion.

For non-canonical orientations, we rotate images in 90° increments to approximate a canonical horizontal viewpoint. Other issues, such as point cloud noise and image blur, are mitigated via re-calculating 7-DOF bounding boxes of annotated objects and tailored prompt engineering for 2D MLLMs. Further implementation details are provided in the supplementary material.

3.3. Data Curation Pipeline

For scene acquisition, we compile 25 K scans from five datasets: ScanNet [11], CA-1M [19], 3RScan [31], Structured3D [44] (training), and ScanNet++ [39] (testing), cov-

ering both real and synthetic environments. The subsequent curation pipeline consists of four stages.

Meta-annotation collection. Generally, we prompt our in-house MLLMs and LLMs to produce object-, frame-, and scene-level captions during this step. The specific steps are as follows.

- *Frame sampling.* To reduce latency and token cost, we subsample each scan. Video sequences are uniformly sampled; the frames from non-video sequences (e.g. 3RScan) are clustered by camera pose, and one representative frame is retained per cluster.
- *Caption annotation.* For scenes & frames, we prompt MLLM with given images and instructions, while max-coverage sampling [43] caps the number of frames used for the scene caption. For objects, we rank viewpoints by (i) the 2D distance from the object center to the image center and (ii) the visible area ratio obtained by rendering the annotated mesh. The top-2 views are cropped and sent to the MLLM for captioning; an LLM then extracts appearance attributes.

Scene Graph Construction. Following SceneVerse [18], we approximate object occupancy with 3D bounding boxes and build an object-centric graph that records only vertical adjacency and horizontal contact. To suppress noise and ambiguity, we discard multi-object relations (involving more than two nodes) and all relative directions (e.g., left/right or clock-face positions).

Rule-based heuristics cannot identify subtle cases such as “inside” or “hanging from”. We therefore introduce a *Relation Correction* stage, illustrated in Fig. 4a. An MLLM first narrates the interaction between co-visible objects in free text; an R1-style LLM [14] then parses each sentence into one of the predefined relation templates, updating the initial graph accordingly.

Discriminative Object Referring. To mimic the referential adjustments that emerge naturally in human conversation, we exploit the object-level annotations and scene graphs acquired earlier to produce concise, distinguishing descriptions that separate each target from its distractors (Fig. 4b). The proposed method consists of the following three steps to assign non-conflicting referring expressions to similar objects (see cases in Fig. 5).

- *Distractor Grouping:* Objects are clustered by categorical relatedness. Using the label graph as prior, an object is added to a group when its label is identical to, or a hyponym of, the group label. This step isolates the set of objects that can plausibly be confused with one another.
- *Comparative disambiguation.* For every distractor group, we derive a minimal set of modifiers as the initial dis-

criminative object referrals (see the pseudocode in Algorithm 1).

1 *Multi-aspect comparison*: For the appearance dimension, LLM is prompted with few-shot examples to cluster objects by attribute differences. We provide few-shot labeling examples in the prompt to guide the model’s annotation behavior and verify that LLM’s formatted output meets the requirements. For the size dimension, 7-DOF box volumes are compared; a generous tolerance compensates for box–object mismatch. For the object relation dimension, object-centric sub-scene graphs are contrasted to extract distinctive relations.

2 *Descriptor fusion*: We combine the results from these dimensions to obtain G_{all} , which represents the subset of objects that match the descriptors. Given G_{all} , we can derive exclusive and compact descriptive modifiers for each object, distinguishing it from others without any redundant descriptors (see Algorithm 1, lines 9–END).

3 *Singleton fallback*: For objects without distractors, we use their captions or labels directly. The resulting descriptors are rewritten by LLM to reduce template bias.

- *Spatially anchoring*: To incorporate richer 3D context, we introduce two anchors: the *anchor object* and *anchor sight*. For each distractor group, we identify the nearest (or farthest) object relative to the anchor object, and the leftmost (or rightmost) object relative to the anchor sight connecting two objects. All objects serving as references are sampled from non-distractor objects that have already been assigned discriminative object referrals by Comparative disambiguation. Spatial clauses are first templated, then rewritten by LLM for fluency; supplementary material gives full implementation details.

Multi-Task Data Generation. As Fig. 3 shows, our data curation pipeline yields three caption tasks: *scene caption*, *object caption*, and *view caption*. The *view caption* task requires 3D MLLMs to summarize the visible content with the given camera pose and intrinsics. Discriminative object referrals feed the *visual grounding*.

For QA, we define five subtasks: *object size*, *absolute distance*, *relative distance*, *object count*, and *attribute recognition* to cover the all-around spatial understanding capabilities. All questions are instantiated from templates using discriminative object referrals. For the *attribute recognition* task, we restrict the object referral to either the semantic label of the queried object (when no distractors are present) or a spatially anchored object referral, thereby eliminating any risk of answer leakage. This QA task subsumes two formats: True-False items and open-ended

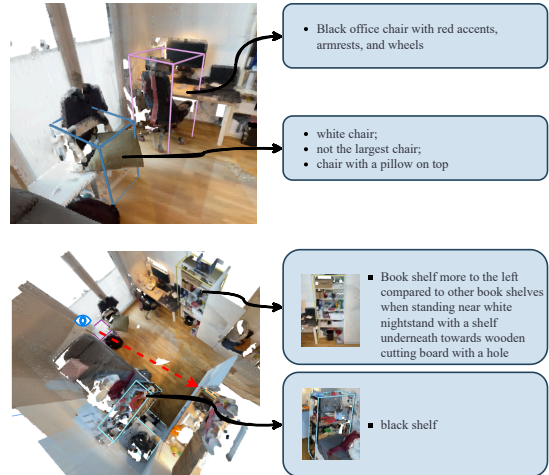


Figure 5. Discriminative object referral examples in ScanNet++ [39] scans.

queries. For the True-False item with the wrong attribute, a plausible yet incorrect property is generated by prompting LLM for the queried object. To compute the distance between two objects for relevant QA tasks, we sample a dense set of points from the surface of 7-DOF bounding boxes. The distance is then defined as the minimum Euclidean distance between these two point sets. Further details are provided in the supplementary material.

3.4. Statistics & Analysis

Overview. As illustrated in Fig. 3, the Disc3D dataset aggregates 25 K scans drawn from simulated and real-world sources. With an automated curation pipeline, we generate multi-million 3D scene dialogues in a matter of days; this count is by no means the pipeline’s ceiling. We perform sampling to ensure a balanced distribution across different QA sub-tasks. To prevent dialogues of complex scenes from dominating the dataset, we impose limits on the number of QA instances generated per scene.

Comparison with existing large-scale 3D multi-modal datasets. MMScan [22] and SceneVerse [18] assemble large-scale 3D multi-modal datasets with human-in-the-loop pipelines. Disc3D eliminates manual effort by replacing annotators with a rule-based engine powered by MLLMs and LLMs. The resulting corpus spans more scenes and samples than MMScan and subsumes the task diversity of SceneVerse. Like MMScan, Disc3D provides scene- and region-level captioning, visual grounding, and multi-dimensional QA. We extend this set with view-level captioning derived from individual frames. Throughout data curation, we eliminated viewpoint ambiguities intro-

Dataset	Samples	Scans	Viewpoint-ambiguity-free	Human-annotation-free	Object Referral Constraint	Task Diversity
SceneVerse [18]	2.5M	68K	No	No	No	★
MMScan [22]	1.45M	5.2K	No	No	No	★ ★ ☆
Disc3D, ours	2.08M	25K	Yes	Yes	Discriminative	★ ★ ★

Table 1. Comparison with two other large-scale 3D MLLM multi-task datasets. Disc3D autonomously curates a two-million-sample multi-task corpus by means of Discriminative Object Referencing, a carefully engineered module that injects contextual constraints into object descriptions and eliminates ambiguities in object identification and spatial relations. Earlier 3D vision-language datasets [1, 3, 23, 42], being smaller and task-specific, still remain vulnerable to ambiguity; they are therefore excluded from direct comparison.

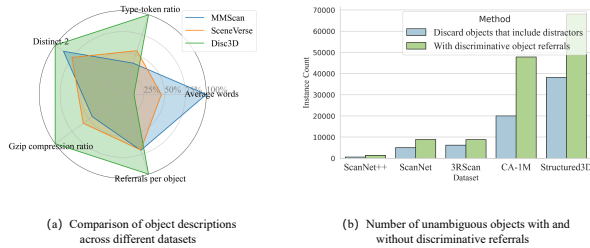


Figure 6. Analysis of object referrals. (a) Our Disc3D incrementally enriches object references, incorporating textual modifiers chosen along carefully controlled dimensions, and thereby yields concise, information-rich object descriptions. The gzip compression ratio plotted is the ratio of the compressed size (bytes) to the original size. (b) By explicitly modeling distractors, Discriminative Object Referring utilizes more object annotations in each source dataset in the absence of referential ambiguity.

duced by either manual design or LLM-generated text. To resolve object-referring ambiguity, we propose Comparative Disambiguation and Spatial Anchoring, which embed discriminative constraints into object descriptions. A brief comparison is provided in Tab. 1.

Analysis of Object Referral. When no referential ambiguity exists, a trivial baseline simply discards any object that has distractors, thereby avoiding confusion but wasting most annotations. In contrast, our *Discriminative Object Referring* strategy lets the curation pipeline retain a substantially larger subset of annotated objects from the source dataset (Fig. 6b). Moreover, compared with MMScan and SceneVerse, Disc3D generates for each object a richer yet concise collection of object descriptions (Fig. 6a).

Human Revision for Test Split. For the Disc3D test split, we conducted manual quality inspection and correction to evaluate the accuracy of object referrals. Since spatially anchored descriptions introduce minimal noise but exhibit low manual annotation accuracy, we focused on verifying object descriptions generated in the *Comparative Disambiguation* stage. Specifically, annotators compared the 2D

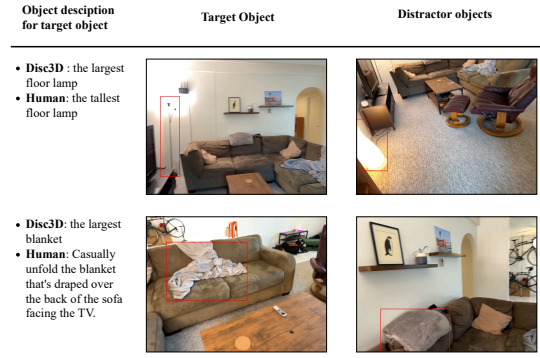


Figure 7. Comparison of object descriptions before and after manual modification.

and 3D views of target and distractor objects to assess the factual accuracy and exclusiveness of the provided descriptions, revising any inaccuracies.

In total, 12% of the descriptions (130/1092) were revised. As illustrated in Fig. 7, the majority of edits introduced by human annotators do not rectify factual inaccuracies but instead refine imprecise wording. For instance, limited descriptors such as “largest” or “smallest” often inadequately capture the distinctive size characteristics of irregularly shaped objects (e.g., floor lamps) or soft, deformable items (e.g., blankets). We contend that such imprecisions, though potentially influencing model preferences, are comparatively tolerable relative to factual errors or ambiguous expressions. Given that manually annotated benchmarks still exhibit non-negligible noise—e.g., human re-evaluation in [16] reports only 62% and 80% accuracy on ScanQA and SQA3D, respectively—Disc3D provides 3D multi-modal data with comparatively low label noise.

Finally, the manually corrected descriptions replaced the original ones for all subsequent processing, yielding the final benchmark of Disc3D.

4. Experiments

We evaluate on two canonical 3D scene-understanding tasks. (1) **3D visual grounding** localises the object

Type	Method	Disc3D-QA					ScanQA (val) (EM/EM-R)	SQA3D (test) (EM/EM-R)
		Absolute Distance	Attribute Recognition	Relative Distance	Object Size	Object Count		
2D-MLLM	InternVL3-8B [46]	0.223	0.649	0.478	0.235	0.250	–	–
	InternVL3-14B	0.226	0.708	0.367	0.352	0.253	–	–
	InternVL3-38B	0.193	0.711	0.555	0.362	0.396	–	–
	InternVL3-78B	0.202	0.702	0.486	0.345	0.344	–	–
3D MLLM	Ross3D [32]	0.106	0.672	0.529	0.181	0.232	0.308 / –	0.630 / 0.657
	Video-3DLLM [43]	0.150	0.638	0.211	0.002	0.188	0.301 / –	0.586 / –
	LLaVA-3D [45]	0.071	0.590	0.514	0.046	0.580	– / 0.306	– / 0.601
	LLaVA-3D, ours	0.299	0.874	0.730	0.505	0.440	0.272 / 0.446	0.600 / 0.629

Table 2. Performances of different 2D MLLMs and 3D MLLMs on the Disc3D QA benchmark and other public 3D-QA benchmarks. We re-implement LLaVA-3D with InternVL3-8B as base model. Our Disc3D training corpus equips LLaVA-3D with consistent gains across multiple axes, as verified on the proposed Disc3D-QA suite and two public benchmarks. Although we deliberately excluded object-counting samples to mitigate dataset bias, the trained model still generalizes well to this task.

described by a natural-language utterance. Asking 3D MLLMs to regress a 3D bounding box in text space is unreliable. We therefore benchmark proposal-matching methods [32, 43] that recast the task as proposal classification: the model aligns predicted grounding tokens with 3D proposals extracted by an off-the-shelf detector [29] at the feature level. We report accuracy on the Disc3D grounding split with 2790 samples and analyse performance under varying conditions. (2) **3D question answering** uses a linear, objective metric that cleanly reflects different facets of model capability; consequently, our main experiments and ablations centre on QA. Benchmarks include the public datasets [3, 23] and the Disc3D multi-dimensional QA suite. The Disc3D-QA test set contains 1 000 questions per category across five dimensions; object counts are unavailable at training time, making this sub-task zero-shot for our model.

Metrics. For visual grounding, we report exact-match accuracy: we use ground-truth object boxes as proposals, thereby removing any confounding effect of localization error. For question-answering, we adopt top-1 exact-match (EM) and its relaxed variant (EM-R) for normal questions, and Mean Relative Accuracy [37] (MRA) for numerical questions such as object size and absolute distance.

Implementation Details. We re-implement LLaVA-3D [45] on InternVL3 [46] and fine-tune the MLP projector and LLM part. For our main experiments and ablations, leveraging its compact end-to-end design and competitive efficiency. In addition to Disc3D, we combine 220 K samples from public datasets to enlarge diversity and enable direct comparison with prior work (see Tab. 4). To balance

Distractors	Objetc Reference	Accuracy (%)	
		Video-3D-LLM [43]	Ross3D [32]
No	Normal	47.5	50.7
Yes	Discriminative	27.3	28.7
	+ Anchor context	14.2	14.5

Table 3. Impact of category-similar distractors and referring-expression type on Disc3D grounding accuracy (proposal-matching methods). “Discriminative” referral encodes object size, spatial relation, and appearance (Comparative Disambiguation). “+Anchor” appends anchor-context to the expression (Spatially Anchoring).

cost and coverage we sample at most 32 frames per scene with max-coverage sampling [43]; all images are centred-cropped to 336×336 pixels.

3D MLLMs on the Disc3D visual-grounding task As Tab. 3 shows, even with perfect localization, both Video-3D-LLM and Ross3D incur large accuracy drops as soon as distractors are present. Under the discriminative object-referral protocol, performance deteriorates further when the referring expression embeds richer spatial context generated by Spatially Anchoring.

Effect of Disc3D as training data. Training on the open-source corpus alone (220K samples, Tab. 4) is compared with the same schedule augmented by Disc3D-QA. To control for compute, the total number of iterations is fixed. Tab. 5 shows that Disc3D brings consistent gains on both ScanQA and SQA3D.

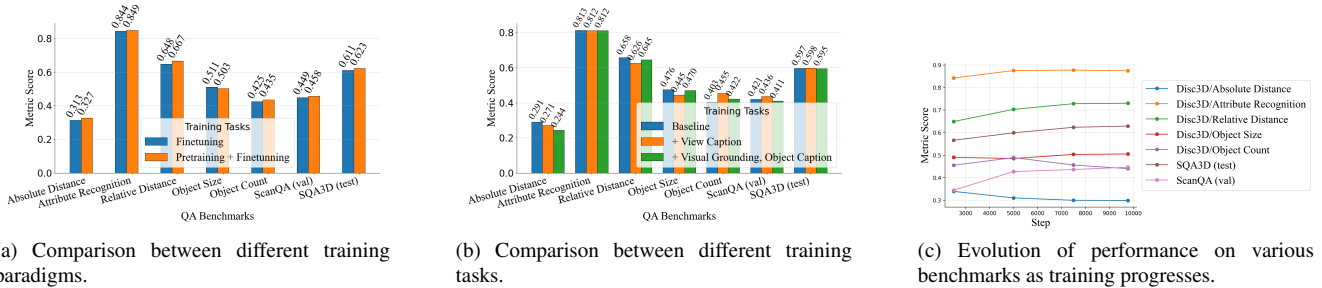


Figure 8. Results for ablation study. (a) Two-stage training yields consistent gains across most benchmarks; (b) Joint training with multi-task data improves the zero-shot performance on the object-counting task. (c) With the full Disc3D-QA dataset for fine-tuning, performance on most benchmarks rises with additional training steps, except for two numeric estimation tasks.

Dataset	Task	Size	Filtered
MMScan	RegionCaption	4724	Yes
MMScan	QA	115072	Yes
SQA3D	QA	79445	No
ScanQA	QA	19046	Yes

Table 4. Details of the 220K public dataset. We clean the dataset by applying keyword filters to remove samples exhibiting potential viewpoint ambiguity. SQA3D dataset is not cleaned, as its *SituatedQA* task inherently encodes positional and viewpoint information within the context.

Model Size	Training Data	ScanQA (val)	SQA3D (test)
2B	Public 220K	0.312	0.569
	+ Disc3D-QA	0.421	0.597
8B	Public 220K	0.405	0.600
	+ Disc3D-QA	0.449	0.611

Table 5. Impact of augmenting the training set with Disc3D under a 1 : 1 mixture and equal iteration steps. The results are evaluated under the refined exact-match protocol.

Impact of Task-Mixing. Fig. 8b reports the QA performance of LLaVA-3D-2B trained with different Disc3D task mixtures. Only the object-count task benefits; all other auxiliary tasks yield no systematic improvement.

Training Paradigm. We compare single-stage fine-tuning with a two-stage scheme on LLaVA-3D-8B. In the first stage, the MLP projector is warmed up on Disc3D-1M, constructed by balanced multi-task sampling from Disc3D. In the second stage, projector and LLM are updated jointly. Fig. 8a shows that the two-stage approach outperforms the single-stage baseline.

Evaluation of 2D & 3D MLLMs on Disc3D-QA. We evaluate 2D and 3D MLLMs on each sub-task of Disc3D-QA. Larger 2D MLLMs improve on most questions, yet remain at chance for *absolute* and *relative distance* without 3D priors. For 3D MLLMs, current SOTA methods still under-perform in the zero-shot evaluation on Disc3D-QA. We observe that Video-3D-LLM underperform random guessing (50%) on the multiple-choice task — *relative distance* — because they fail to select an answer from the provided options (i.e. A/B). Fine-tuning on Disc3D lifts LLaVA-3D across all tasks.

Training Dynamics on the Full Disc3D-QA Corpus Two-stage instruction tuning of LLaVA-3D-8B is run on the full QA corpus; multi-benchmark scores are logged in the second stage. Fig. 8c shows steady gains on Disc3D *attribute recognition* and *relative distance*, mirrored by ScanQA and SQA3D. Object-count and the metric-estimation tasks plateau; the former lacks training examples, the latter suffers from sparse numeric supervision and coarse scene encoding (patch-centre coordinates + voxel pooling).

5. Limitations and Conclusion

We propose *Discriminative Object Referring* to simulate realistic object-referring across multiple aspects in dialogues. Our framework resolves ambiguities present in earlier datasets while raising task difficulty. Without manual annotation, we curate Disc3D dataset of million samples spanning 25K scans.

Experiments demonstrate that training on our Disc3D significantly enhances QA performance on the benchmark across all metrics and yields consistent gains on public benchmarks. Current 3D MLLMs nevertheless remain weak in metric-estimation tasks, hindered by under-developed 3D vision encoders and more powerful 3D MLLM designs. Further progress demands co-evolution of architectures and data.

References

- [1] Panos Achlioptas, Ahmed Abdelreheem, Fei Xia, Mohamed Elhoseiny, and Leonidas Guibas. Referit3d: Neural listeners for fine-grained 3d object identification in real-world scenes. In *European conference on computer vision*, pages 422–440. Springer, 2020. 1, 2, 6
- [2] Armen Avetisyan, Christopher Xie, Henry Howard-Jenkins, Tsun-Yi Yang, Samir Aroudj, Suvam Patra, Fuyang Zhang, Duncan Frost, Luke Holland, Campbell Orme, et al. Scene-script: Reconstructing scenes with an autoregressive structured language model. In *European Conference on Computer Vision*, pages 247–263. Springer, 2024. 2
- [3] Daichi Azuma, Taiki Miyanishi, Shuhei Kurita, and Motoaki Kawanabe. Scanqa: 3d question answering for spatial scene understanding. In *proceedings of the IEEE/CVF conference on computer vision and pattern recognition*, pages 19129–19139, 2022. 1, 2, 6, 7
- [4] Shuai Bai, Keqin Chen, Xuejing Liu, Jialin Wang, Wenbin Ge, Sibao Song, Kai Dang, Peng Wang, Shijie Wang, Jun Tang, et al. Qwen2. 5-vl technical report. *arXiv preprint arXiv:2502.13923*, 2025. 2
- [5] Gilad Baruch, Zhuoyuan Chen, Afshin Dehghan, Tal Dimry, Yuri Feigin, Peter Fu, Thomas Gebauer, Brandon Joffe, Daniel Kurz, Arik Schwartz, et al. Arkitscenes: A diverse real-world dataset for 3d indoor scene understanding using mobile rgb-d data. *arXiv preprint arXiv:2111.08897*, 2021. 2
- [6] Mohamed El Amine Boudjoghra, Angela Dai, Jean Lahoud, Hisham Cholakkal, Rao Muhammad Anwer, Salman Khan, and Fahad Shahbaz Khan. Open-yolo 3d: Towards fast and accurate open-vocabulary 3d instance segmentation. *arXiv preprint arXiv:2406.02548*, 2024. 1
- [7] Angel Chang, Angela Dai, Thomas Funkhouser, Maciej Halber, Matthias Niessner, Manolis Savva, Shuran Song, Andy Zeng, and Yinda Zhang. Matterport3d: Learning from rgb-d data in indoor environments. *arXiv preprint arXiv:1709.06158*, 2017. 2
- [8] Dave Zhenyu Chen, Angel X Chang, and Matthias Nießner. Scanrefer: 3d object localization in rgb-d scans using natural language. In *European conference on computer vision*, pages 202–221. Springer, 2020. 1, 2
- [9] Sijin Chen, Xin Chen, Chi Zhang, Mingsheng Li, Gang Yu, Hao Fei, Hongyuan Zhu, Jiayuan Fan, and Tao Chen. Ll3da: Visual interactive instruction tuning for omni-3d understanding reasoning and planning. In *Proceedings of the IEEE/CVF conference on computer vision and pattern recognition*, pages 26428–26438, 2024. 2
- [10] Zhenyu Chen, Ronghang Hu, Xinlei Chen, Matthias Nießner, and Angel X Chang. Unit3d: A unified transformer for 3d dense captioning and visual grounding. In *Proceedings of the IEEE/CVF international conference on computer vision*, pages 18109–18119, 2023. 2
- [11] Angela Dai, Angel X. Chang, Manolis Savva, Maciej Halber, Thomas Funkhouser, and Matthias Nießner. Scannet: Richly-annotated 3d reconstructions of indoor scenes. In *Proc. Computer Vision and Pattern Recognition (CVPR)*, IEEE, 2017. 2, 4
- [12] Matt Deitke, Eli VanderBilt, Alvaro Herrasti, Luca Weihs, Jordi Salvador, Kiana Ehsani, Winson Han, Eric Kolve, Ali Farhadi, Aniruddha Kembhavi, and Roozbeh Mottaghi. ProcTHOR: Large-Scale Embodied AI Using Procedural Generation. In *NeurIPS*, 2022. Outstanding Paper Award. 2
- [13] Jiajun Deng, Tianyu He, Li Jiang, Tianyu Wang, Feras Dayoub, and Ian Reid. 3d-llava: Towards generalist 3d llms with omni superpoint transformer. In *Proceedings of the Computer Vision and Pattern Recognition Conference*, pages 3772–3782, 2025. 2
- [14] Daya Guo, Dejian Yang, Haowei Zhang, Junxiao Song, Ruoyu Zhang, Runxin Xu, Qihao Zhu, Shirong Ma, Peiyi Wang, Xiao Bi, et al. Deepseek-r1: Incentivizing reasoning capability in llms via reinforcement learning. *arXiv preprint arXiv:2501.12948*, 2025. 4
- [15] Haifeng Huang, Yilun Chen, Zehan Wang, Rongjie Huang, Runsen Xu, Tai Wang, Luping Liu, Xize Cheng, Yang Zhao, Jiangmiao Pang, et al. Chat-scene: Bridging 3d scene and large language models with object identifiers. *Advances in Neural Information Processing Systems*, 37: 113991–114017, 2024. 2
- [16] Jiangyong Huang, Baoxiong Jia, Yan Wang, Ziyu Zhu, Xiongkun Linghu, Qing Li, Song-Chun Zhu, and Siyuan Huang. Unveiling the mist over 3d vision-language understanding: Object-centric evaluation with chain-of-analysis. In *Proceedings of the IEEE/CVF Conference on Computer Vision and Pattern Recognition (CVPR)*, 2025. 6
- [17] Pin-Hao Huang, Han-Hung Lee, Hwann-Tzong Chen, and Tyng-Luh Liu. Text-guided graph neural networks for referring 3d instance segmentation. In *Proceedings of the AAAI Conference on Artificial Intelligence*, pages 1610–1618, 2021. 2
- [18] Baoxiong Jia, Yixin Chen, Huangyue Yu, Yan Wang, Xuesong Niu, Tengyu Liu, Qing Li, and Siyuan Huang. Sceneverse: Scaling 3d vision-language learning for grounded scene understanding. In *European Conference on Computer Vision*, pages 289–310. Springer, 2024. 2, 4, 5, 6, 3
- [19] Justin Lazarow, David Griffiths, Gefen Kohavi, Francisco Crespo, and Afshin Dehghan. Cubify anything: Scaling indoor 3d object detection. In *Proceedings of the Computer Vision and Pattern Recognition Conference*, pages 22225–22233, 2025. 4, 1
- [20] Aixin Liu, Bei Feng, Bing Xue, Bingxuan Wang, Bochao Wu, Chengda Lu, Chenggang Zhao, Chengqi Deng, Chenyu Zhang, Chong Ruan, et al. Deepseek-v3 technical report. *arXiv preprint arXiv:2412.19437*, 2024. 4, 1
- [21] Junyu Luo, Jiahui Fu, Xianghao Kong, Chen Gao, Haibing Ren, Hao Shen, Huaxia Xia, and Si Liu. 3d-sps: Single-stage 3d visual grounding via referred point progressive selection. In *Proceedings of the IEEE/CVF Conference on Computer Vision and Pattern Recognition*, pages 16454–16463, 2022. 2
- [22] Ruiyuan Lyu, Jingli Lin, Tai Wang, Xiaohan Mao, Yilun Chen, Runsen Xu, Haifeng Huang, Chenming Zhu, Dahua Lin, and Jiangmiao Pang. Mmscan: A multi-modal 3d

- scene dataset with hierarchical grounded language annotations. *Advances in Neural Information Processing Systems*, 37:50898–50924, 2024. 1, 2, 5, 6, 3
- [23] Xiaojian Ma, Silong Yong, Zilong Zheng, Qing Li, Yitao Liang, Song-Chun Zhu, and Siyuan Huang. Sqa3d: Situated question answering in 3d scenes. *arXiv preprint arXiv:2210.07474*, 2022. 1, 2, 6, 7
- [24] Arjun Majumdar, Anurag Ajay, Xiaohan Zhang, Pranav Putta, Sriram Yenamandra, Mikael Henaff, Sneha Silwal, Paul Mcvay, Oleksandr Maksymets, Sergio Arnaud, Karmesh Yadav, Qiyang Li, Ben Newman, Mohit Sharma, Vincent Berges, Shiqi Zhang, Pulkit Agrawal, Yonatan Bisk, Dhruv Batra, Mrinal Kalakrishnan, Franziska Meier, Chris Paxton, Sasha Sax, and Aravind Rajeswaran. Openeqa: Embodied question answering in the era of foundation models. In *Conference on Computer Vision and Pattern Recognition (CVPR)*, 2024. 2
- [25] Yongsen Mao, Yiming Zhang, Hanxiao Jiang, Angel X Chang, and Manolis Savva. Multiscan: Scalable rgb-d scanning for 3d environments with articulated objects. In *Advances in Neural Information Processing Systems*, 2022. 2
- [26] Zhangyang Qi, Ye Fang, Zeyi Sun, Xiaoyang Wu, Tong Wu, Jiaqi Wang, Dahua Lin, and Hengshuang Zhao. Gpt4point: A unified framework for point-language understanding and generation. In *Proceedings of the IEEE/CVF conference on computer vision and pattern recognition*, pages 26417–26427, 2024. 2
- [27] Zhangyang Qi, Zhixiong Zhang, Ye Fang, Jiaqi Wang, and Hengshuang Zhao. Gpt4scene: Understand 3d scenes from videos with vision-language models. *arXiv preprint arXiv:2501.01428*, 2024. 2
- [28] Santhosh Kumar Ramakrishnan, Aaron Gokaslan, Erik Wijmans, Oleksandr Maksymets, Alexander Clegg, John M Turner, Eric Undersander, Wojciech Galuba, Andrew Westbury, Angel X Chang, Manolis Savva, Yili Zhao, and Dhruv Batra. Habitat-matterport 3d dataset (HM3d): 1000 large-scale 3d environments for embodied AI. In *Thirty-fifth Conference on Neural Information Processing Systems Datasets and Benchmarks Track*, 2021. 2
- [29] Jonas Schult, Francis Engelmann, Alexander Hermans, Or Litany, Siyu Tang, and Bastian Leibe. Mask3d: Mask transformer for 3d semantic instance segmentation. *arXiv preprint arXiv:2210.03105*, 2022. 7
- [30] Kimi Team, Angang Du, Bohong Yin, Bowei Xing, Bowen Qu, Bowen Wang, Cheng Chen, Chenlin Zhang, Chenzhuang Du, Chu Wei, et al. Kimi-vl technical report. *arXiv preprint arXiv:2504.07491*, 2025. 2
- [31] Johanna Wald, Armen Avetisyan, Nassir Navab, Federico Tombari, and Matthias Nießner. Rio: 3d object instance re-localization in changing indoor environments. In *Proceedings of the IEEE/CVF International Conference on Computer Vision*, pages 7658–7667, 2019. 2, 4
- [32] Haochen Wang, Yucheng Zhao, Tiancai Wang, Haoqiang Fan, Xiangyu Zhang, and Zhaoxiang Zhang. Ross3d: Reconstructive visual instruction tuning with 3d-awareness. *arXiv preprint arXiv:2504.01901*, 2025. 7
- [33] Yanmin Wu, Xinhua Cheng, Renrui Zhang, Zesen Cheng, and Jian Zhang. Eda: Explicit text-decoupling and dense alignment for 3d visual grounding. In *Proceedings of the IEEE/CVF conference on computer vision and pattern recognition*, pages 19231–19242, 2023. 2
- [34] Zhiyu Wu, Xiaokang Chen, Zizheng Pan, Xingchao Liu, Wen Liu, Damai Dai, Huazuo Gao, Yiyang Ma, Chengyue Wu, Bingxuan Wang, et al. Deepseek-vl2: Mixture-of-experts vision-language models for advanced multimodal understanding. *arXiv preprint arXiv:2412.10302*, 2024. 2
- [35] Runsen Xu, Zhiwei Huang, Tai Wang, Yilun Chen, Jiangmiao Pang, and Dahua Lin. Vlm-grounder: A vlm agent for zero-shot 3d visual grounding. *arXiv preprint arXiv:2410.13860*, 2024. 2
- [36] Runsen Xu, Xiaolong Wang, Tai Wang, Yilun Chen, Jiangmiao Pang, and Dahua Lin. Pointllm: Empowering large language models to understand point clouds. In *European Conference on Computer Vision*, pages 131–147. Springer, 2024. 2
- [37] Jihan Yang, Shusheng Yang, Anjali W Gupta, Rilyn Han, Li Fei-Fei, and Saining Xie. Thinking in space: How multimodal large language models see, remember, and recall spaces. In *Proceedings of the Computer Vision and Pattern Recognition Conference*, pages 10632–10643, 2025. 1, 2, 7
- [38] Zhengyuan Yang, Songyang Zhang, Liwei Wang, and Jiebo Luo. Sat: 2d semantics assisted training for 3d visual grounding. In *Proceedings of the IEEE/CVF International Conference on Computer Vision*, pages 1856–1866, 2021. 2
- [39] Chandan Yeshwanth, Yueh-Cheng Liu, Matthias Nießner, and Angela Dai. Scannet++: A high-fidelity dataset of 3d indoor scenes. In *Proceedings of the International Conference on Computer Vision (ICCV)*, 2023. 4, 5
- [40] Hanxun Yu, Wentong Li, Song Wang, Junbo Chen, and Jianke Zhu. Inst3d-llm: Instance-aware 3d scene understanding with multi-modal instruction tuning. In *Proceedings of the Computer Vision and Pattern Recognition Conference*, pages 14147–14157, 2025. 2
- [41] Zhihao Yuan, Xu Yan, Yinghong Liao, Ruimao Zhang, Sheng Wang, Zhen Li, and Shuguang Cui. Instancerefer: Cooperative holistic understanding for visual grounding on point clouds through instance multi-level contextual referring. In *Proceedings of the IEEE/CVF International Conference on Computer Vision*, pages 1791–1800, 2021. 2
- [42] Yiming Zhang, ZeMing Gong, and Angel X Chang. Multi3drefer: Grounding text description to multiple 3d objects. In *Proceedings of the IEEE/CVF International Conference on Computer Vision*, pages 15225–15236, 2023. 1, 2, 6
- [43] Duo Zheng, Shijia Huang, and Liwei Wang. Video-3d llm: Learning position-aware video representation for 3d scene understanding. In *Proceedings of the Computer Vision and Pattern Recognition Conference*, pages 8995–9006, 2025. 2, 4, 7
- [44] Jia Zheng, Junfei Zhang, Jing Li, Rui Tang, Shenghua Gao, and Zihan Zhou. Structured3d: A large photo-realistic dataset for structured 3d modeling. In *European Conference on Computer Vision*, pages 519–535. Springer, 2020. 4, 1
- [45] Chenming Zhu, Tai Wang, Wenwei Zhang, Jiangmiao Pang, and Xihui Liu. Llava-3d: A simple yet effective pathway

to empowering lmms with 3d-awareness. *arXiv preprint arXiv:2409.18125*, 2024. [2](#), [7](#)

- [46] Jinguo Zhu, Weiyun Wang, Zhe Chen, Zhaoyang Liu, Shenglong Ye, Lixin Gu, Hao Tian, Yuchen Duan, Weijie Su, Jie Shao, et al. Internvl3: Exploring advanced training and test-time recipes for open-source multimodal models. *arXiv preprint arXiv:2504.10479*, 2025. [7](#)
- [47] Ziyu Zhu, Xiaojian Ma, Yixin Chen, Zhidong Deng, Siyuan Huang, and Qing Li. 3d-vista: Pre-trained transformer for 3d vision and text alignment. In *Proceedings of the IEEE/CVF International Conference on Computer Vision*, pages 2911–2921, 2023. [2](#)

Disc3D: Automatic Curation of High-Quality 3D Dialog Data via Discriminative Object Referring

Supplementary Material

6. Details in Data Curation Pipeline

6.1. 7-DOF Bounding Box Annotation

As discussed in the main text, the 9-DOF bounding box is sensitive to point-cloud noise, which degrades subsequent distance and collision estimation and complicates model learning. As Algorithm 2, we therefore refit 7-DOF bounding boxes using the provided point-cloud annotations. In Disc3D, the z-axis of every scan is already aligned with gravity, eliminating the need for explicit gravity-direction estimation. For certain source datasets (e.g., Structured3D, CA-1M) they omit per-object point-cloud labels, but directly provided 7-DOF 3D bounding boxes.

6.2. Label Graph Construction

To construct the label graph, we adopt DeepSeek-V3 [20] as the oracle for deciding subsumption between object labels. The query template is:

You are an expert in indoor/outdoor object categorization. Answer YES or NO: the category “{label1}” is a subclass of “{label2}”.

6.3. Details of Source Dataset Processing

Beyond the issues discussed in the main text, several datasets require additional handling:

- Class-agnostic annotations in CA-1M.** CA-1M [19] provides object annotation without semantic labels. During the Object-Caption stage, we prompt a 2D MLLM with the object views and ask it to predict the class label, following the NYU-40 taxonomy.
- Invalid scenes in Structured3D.** We filter out the scenes listed in the official error list. We further discard any image whose mean intensity exceeds a brightness threshold, thereby removing over-exposed views. Specifically, for each image, we compute the fraction of uint8 pixels whose gray-level intensity exceeds 245. If this fraction surpasses 90%, the image is labeled as over-exposed. Following this criterion, we discard 143 over-exposed scenes from Structured3D [44]; representative examples are shown in Figure 9.
- Missing segmentation labels in CA-1M.** Because CA-1M [19] lacks 2D and 3D segmentation, we estimate object visibility masks used in the caption annotation procedure heuristically. Inspired by OpenYolo3D [6], we combine depth values with the provided 2D bounding boxes to construct a per-frame label map. For each image, we compute the average depth inside every bound-

Algorithm 2 Compute 7-DoF Oriented Bounding Box

Input: A object point cloud $P = \{(x_i, y_i, z_i)\}_{i=1}^N$.

Output: A 7-DoF bounding box: center C , size S , and yaw angle yaw_L .

```
1: if  $|P| < 3$  then
2:   # Fallback to Axis-Aligned Bounding Box for few points
3:    $(C, S) \leftarrow \text{AABB}(P)$ 
4:    $\text{yaw}_L \leftarrow 0$ 
5:   return  $(C, S, \text{yaw}_L)$ 
6: end if
7: # Step 1: Project points onto the XY plane
8:  $P_{xy} \leftarrow \{(x_i, y_i) \mid (x_i, y_i, z_i) \in P\}$ 
9: # Step 2: Compute Minimum Area Bounding Rectangle (MABR)
10:  $(c_{xy}, (d_1, d_2), \theta_{cv}) \leftarrow \text{MinAreaRect}(P_{xy})$ 
11: # Step 3: Determine the yaw angle from the MABR
12:  $\text{yaw}_{d1} \leftarrow -\text{to\_rad}(\theta_{cv})$ 
13:  $\text{yaw}_{d2} \leftarrow \text{yaw}_{d1} + \pi/2$ 
14: # Assign L, W based on the longer side in the XY plane
15: if  $d_1 \geq d_2$  then
16:    $L \leftarrow d_1, W \leftarrow d_2, \text{yaw}_L \leftarrow \text{normalize\_angle}(\text{yaw}_{d1})$ 
17: else
18:    $L \leftarrow d_2, W \leftarrow d_1, \text{yaw}_L \leftarrow \text{normalize\_angle}(\text{yaw}_{d2})$ 
19: end if
20: # Step 4: Compute center and height along the Z-axis
21:  $z_{\min} \leftarrow \min(\{z_i \mid (x_i, y_i, z_i) \in P\})$ 
22:  $z_{\max} \leftarrow \max(\{z_i \mid (x_i, y_i, z_i) \in P\})$ 
23:  $c_z \leftarrow (z_{\min} + z_{\max})/2$ 
24:  $H \leftarrow z_{\max} - z_{\min}$ 
25: # Assemble the final 7-DoF box parameters
26:  $C \leftarrow (c_{xy}[0], c_{xy}[1], c_z)$ 
27:  $S \leftarrow (L, W, H)$ 
28: return  $(C, S, \text{yaw}_L)$ 
```

ing box, sort the boxes from far to near, and assign object IDs in this order. Consequently, regions of distant objects are covered by nearer ones.

6.4. MLLMs and LLMs for Annotation

In most tasks, we rely on proprietary MLLMs and LLMs for annotation, text rewriting, and other related operations. When the output must follow a specific structure, we include the desired format in the prompt and validate the re-

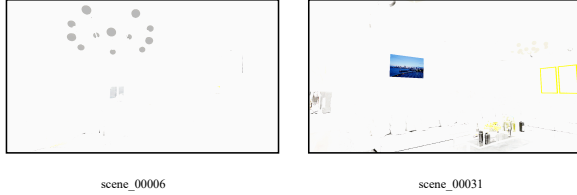


Figure 9. Samples of overexposed images from the Structured3D dataset.

turned result. The prompts for the key steps are provided below for reference (note that the content enclosed in double square brackets serves as a placeholder, awaiting the insertion of external variables at runtime.):

- Prompt for scene annotation: *Given the multiple images of a scene, describe the scene. Note that you must obey the following requirements: 1. Avoid using expressions like 'the image' in the description; 2. Avoid using relative direction words/phrases, such as left/right/front/back; 3. Do not give the specific number of any objects in the image and just use 'multiple'; 4. Be concise and accurate and output no more than 300 words.*
- Prompt for frame annotation: *Describe the scene shown in the image. Note that you must obey the following requirements: 1. Avoid using expressions like 'the image' in the description; 2. Avoid using relative direction words/phrases, such as left/right/front/back; 3. Do not give the specific number of any objects in the image and just use 'multiple'; 4. Be concise and accurate and output no more than 100 words.*
- Prompt for object annotation: *Suppose you are an image annotation assistant, and you will judge whether the "[[ObjectLabel]]" can be seen in the bounding box of given images and describe it. Follow the following rules in one step: 1. Firstly, judge that whether the "[[ObjectLabel]]" can be seen in the bounding box of given images and return YES/NO. 2. If the "[[ObjectLabel]]" can be seen clearly, summarize a precise object description for "[[ObjectLabel]]". Note the following requirements: 1. Avoid using words such as "image/scene" in the answer. 2. Do not include other objects in the answer. 3. Avoid using non-sense words, such as 'unclear', 'unknown', 'unidentified', 'uncertain', 'unpredictable', 'doubtful', 'undetermined', 'unable'.*
- Prompt for relation judgment and re-description of scene graph: *Carefully observe the two objects enclosed by the bounding boxes in the image. Is the [[ObjectA]] [[Relation]] [[ObjectB]] in this picture? Return Yes/No, and if NO, briefly describe the spatial relationship between two objects, with the following requirements: 1. Do not use any descriptions that rely on the current camera perspective, such as 'in front of', 'behind', 'left' or 'right'; 2.*

Algorithm 3 Calculate Signed Angle Between Two 2D Vectors

Input Two 2D vectors $\mathbf{v}_1 = (x_1, y_1)$ and $\mathbf{v}_2 = (x_2, y_2)$.

Output The signed angle θ from \mathbf{v}_1 to \mathbf{v}_2 in radians, where $\theta \in [-\pi, \pi]$.

- 1: dot_product $\leftarrow x_1x_2 + y_1y_2$
 - 2: cross_product $\leftarrow x_1y_2 - y_1x_2$
 - 3: $\theta \leftarrow \text{atan2}(\text{cross_product}, \text{dot_product})$
 - 4: **Return** θ
-

Use the relations in [[Predefined Relations]].

- Prompt for extracting the corrected the relation: *Given the relationship description between objectA "[[ObjectA]]" and objectB "[[ObjectB]]": [[the corrected description of object relations]] Extract the preposition/phrase indicating their relationship, with the following requirements: 1. Return The relationship preposition/phrase only and do not add any other words. 2. The relationship preposition/phrase should satisfy the format: objectA is/are [relationship preposition/phrase] objectB. 3. Avoid using words that depend on the current viewing perspective, such as 'front', 'back', 'behind', 'left' or 'right'*

We refine object-relation extraction by leveraging proprietary reasoning-style LLMs, thereby enhancing accuracy.

6.5. Comparative Disambiguation

For appearance analysis, we leveraged an LLM assistant to extract and compare the color, shape, material, and condition attributes of objects within each distractor set (when available). As Figure 12 shows, these attributes were compiled into markdown tables, and a small set of annotated cases was provided to steer the model toward accurate predictions via in-context learning.

Regarding object size, we assign the labels `largest` and `smallest` to the extreme instances (after accounting for a noise buffer), and `not-largest` and `not-smallest` to all others.

For object relations, within each resulting group, we identify the distinctive relations that distinguish a given object from the remaining members. To suppress noise, we assume that object-centric subgraphs are identical for any object pair whose members lie within 50 cm of each other. To keep the generated description concise, only one distinctive relation is retained.

6.6. Object Distance Estimation

To approximate the distance between two objects, we adopt their 7-DOF bounding boxes as coarse spatial proxies. The procedure is as follows:

1. Detect overlap by applying the Separating Axis Theorem (SAT) to the two boxes. If an overlap is detected, the inter-object distance is set to zero.

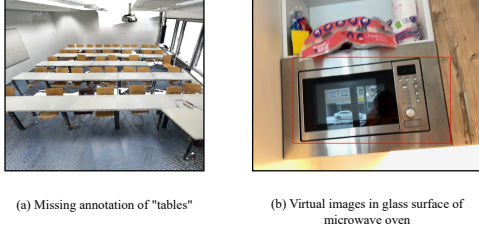


Figure 10. Examples of remaining issues in 3D scene dataset.



Figure 11. Comparison of object descriptions before and after manual modification.

2. Otherwise, sample 16 uniformly distributed points on each face of both boxes and compute all pairwise point-to-point distances; the minimum among these values is taken as the estimated distance between the objects.

6.7. Spatially Anchoring

For Spatially Anchoring, we generate discriminative object descriptions according to the following logic:

1. **Anchor-object sampling:** We sample from the non-distractors of current distractor group, which must lie at least 50 cm from the anchor and compute all pairwise distances between the anchor object and the target. If an object is the furthest or the nearest to the anchor, we assign it the corresponding template-based description. To account for estimation errors in 3D bounding-box distances, we introduce a dynamic noise buffer equal to the maximum dimension among all orientation-aligned bounding boxes in the distractor group.
2. **Anchor-sight sampling:** For objects defining the start and end of the anchor sight, we enforce a minimum separation of 50 cm. To eliminate the effect of height differences, we consider only the XY plane when determining the relative direction between an object and the sightline. For each distractor group, if an object lies at the

extreme right or extreme left of the sightline (within a 10° buffer), we assign the corresponding descriptor. The computation of the object’s relative angle to the sightline is illustrated in Algorithm 3.

6.8. Details for Attribute Recognition QA

As shown in Table 6, for true/false questions in attribute-recognition QA, directly sampling incorrect answers from attributes of other objects in the same category cannot eliminate the influence of semantically similar attributes expressed in different words. Therefore, we employ a large language model (LLM) to generate intentionally misleading wrong answers. As illustrated in Figure 14, we supply the model with the object label, attribute field, and attribute value, guiding the LLM to produce plausible yet non-identical attribute values for that object category. This strategy helps mitigate the shortcut risk in QA tasks — namely, the tendency of the model to infer answers solely from the object type mentioned in the question.

6.9. Question Templates

For Scene Caption & Visual Grounding, the question prompts for the two tasks are generated by LLM for summarizing the room descriptions. Other question templates can be found in Figure 13. For attribute-recognition tasks, the training set comprises both true/false questions and open-ended items, whereas the test set is restricted to true/false questions to enable a more precise evaluation.

6.10. Comparison of Object Descriptions

As shown in Figure 15, we provide a comparison of object descriptions. MMScan [22] and SceneVerse [18] enumerate almost every observable attribute — appearance, location, geometry, functionality, and ancillary details, yielding exhaustive yet lengthy descriptions. Such verbosity, while informative, dilutes the discriminative cues required to unambiguously identify an object. In contrast, our Disc3D pipeline distills a concise, multi-view signature that foregrounds the distinguishing characteristics of each object, thereby offering a more effective dataset for assessing and guiding the spatial understanding capability of 3D MLLMs.

6.11. Remaining Limitations

We addressed a range of defects in the source dataset, including subsumption relations in semantic labels, abnormal camera poses, blurred images, and point-cloud noise. Despite these remedies, two issues remain unresolved.

1. **Missing object annotations.** Dense or poorly delineated objects are often skipped, leading to incomplete labels (see Figure 10(a)).
2. **Reflection and refraction.** Glass surfaces create virtual images that MLLMs incorporate into view-dependent

```

Suppose you are an assistant being good at summarizing the commonality & difference between different object captions.
Follow the next step according to the following rules:
1. You will be given a markdown format table recording the properties of multiple objects.
2. Analyze each column of the table.
3. Group the objects based on the table. The objects in the same group should share the common property that differs with other groups.
4. Summarize the commonality as a adjective or a concise phrase.
5. Return the grouping result as a json format dict.
Note the following requirements:
1. Don't use any vague word, such as unknown, unspecified, unsure, etc.
2. Find the major and discriminative feature to group all the objects.
2. The properties that are similar but not identical are considered the same, including similar color,similar shape, similar placement.
Example 1:
Inputs:

|   | colors                                      | material                       |
|---|---------------------------------------------|--------------------------------|
| 0 | brown (wooden part), light gray (cushion)   | wood (frame), fabric (cushion) |
| 1 | light brown (wooden part), beige (cushion)  | wood (frame), fabric (cushion) |
| 2 | dark gray                                   | wood                           |
| 3 | brown (wooden part), beige (cushioned seat) | wood (frame), fabric (cushion) |
| 4 | brown (wooden part), beige (cushion)        | wood (frame), fabric (cushion) |

Answer: {"brown color": [0, 1, 3, 4], "dark gray": [2]}
Example 2:
Inputs:

|   | color      | placement |
|---|------------|-----------|
| 0 | light gray | draped    |
| 1 | gray       | draped    |

Answer: {"gray": [0, 1]}

```

Figure 12. Prompt for grouping distractors by appearance in the procedure of Comparative Disambiguation.

Question Templates	
View Caption	<p>Given the following camera parameters in the 3D scene:</p> <ul style="list-style-type: none"> - Position: [x, y, z] in world coordinates (cm) - Orientation: (right-handed coordinate system with Z as polar axis): - Azimuth (θ) = [value]$^\circ$ (0$^\circ$: +X axis, increasing counterclockwise in XY plane) - Polar angle (ϕ) = [value]$^\circ$ (0$^\circ$: +Z axis, 90$^\circ$: XY plane, 180$^\circ$: -Z axis) - Field of View: [fov_x, fov_y]$^\circ$ (horizontal and vertical angles in degrees) <p>Predict a descriptive caption for the scene visible through this camera.</p> <p>### Camera Parameters</p> <p>Position: {0}</p> <p>θ: {1}$^\circ$</p> <p>ϕ: {2}$^\circ$</p> <p>FOV: {3}$^\circ$</p>
QA/Absolute Distance	Find the two objects: 1. {0}; 2. {1}. Measuring from the center of each object, what is the distance between the two objects in meters?
QA/Relative Distance	Find the two objects: A. {0}; B. {1}. Which object is {2} the reference object -- {3}?
QA/Attribute Recognition True or False question	Find the object '{0}' in the scene, and answer: can its {1} be described as '{2}'? Please answer strictly with 'yes' or 'no'.
QA/Attribute Recognition Open-Ended	Find the object: '{0}' in the scene, and describe its {1} concisely.

Figure 13. Question templates for multi-task data generation.

descriptions, thereby distorting the 3-D scene understanding (see Figure 10(b)).

7. Disc3D benchmark

We provide Disc3D-QA, the benchmark comprising 5K annotated examples evaluated in the main paper, in the supplementary material.

7.1. Human Annotation for object referrals in Disc3D

As shown in Figure 11, we present representative cases before and after human quality inspection. Factual inaccuracies in descriptions generated by the Comparative Disambiguation module of our Disc3D pipeline (e.g., the fourth row in Figure 11) occur far less frequently than the edits introduced by annotators. A substantial portion of revisions target stylistic or linguistic refinement rather than correct-

Task: Generate a plausible alternative attribute value for a given object label, attribute key, and correct attribute value. The output must be a single possible value (1-2 words) that logically fits the object category and attribute key, distinct from the provided correct value.

Steps:

1. Analyze the object label (e.g., "computer"), attribute key (e.g., "color"), and correct value (e.g., "black").
2. Identify common attribute values associated with the object category and key.
3. Generate one alternative value that is both typical for the category and different from the provided correct value.

Examples:

Input: computer | color | black
Your answer: white

Input: phone | material | plastic
Your answer: metal

Input: car | shape | rectangular
Your answer: aerodynamic

Format Requirements:

- Output ONLY the alternative value (no explanations or punctuation)
- Use lowercase unless brand names/proper nouns are required
- Ensure values are realistic and category-appropriate

Figure 14. The prompt for guiding LLM to generate the distracting object attribute in QA.

Category	Attributes			Distracting Attributes		
	color	material	shape	color	material	shape
curtain	white	-	-	blue	-	-
door	brown	wooden	-	white	metal	-
carpet	black	-	-	gray	-	-
tv	black	-	flat	silver	-	curved
pillow	light-colored	-	square	blue	-	round

Table 6. Comparison between the object attributes and the distracting attributes generated by the LLM

Disc3D/Object Description	MMScan/Object Description	SceneVerse/Object Description
Green curtain	The curtain is a standard, light-colored decoration. It is made of smooth material, either cotton or polyester fiber. The curtain is of moderate size, covering a part of the window or door. It is in good condition, not pulled open. It hangs vertically from the ceiling. The design of the curtain is simple, without any obvious patterns or decorations.	The curtain is a white, rectangular window curtain made of a smooth, fabric material. It has a curvy shape and is used to cover a window. It has a silky texture and a simple structure.
The largest curtain		
Curtain farthest from blue, white, and black striped clothes		
Curtain more to the right compared to other curtains when standing near rectangular mirror with dark frame towards nightstand with book on top		

Figure 15. A comparison of object descriptions across different datasets (using "curtain" as an example).

ness, with a notable share focusing on size descriptors (rows one and two in (e.g., the fourth row in Figure 11)). Simple tokens such as largest or smallest often fail to capture the distinctive size characteristics of objects with irregular shapes (e.g., floor lamps) or soft, deformable items (e.g., blankets).